J Mater Sci (2009) 44:3731–3735
DOI 10.1007/s10853-009-3498-4

Effect of the titanium ion concentration on electrodeposition of nanostructured TiNi films

Hae-Min Lee · Santosh K. Mahapatra · John Kiran Anthony · Fabian Rotermund · Chang-Koo Kim

Received: 7 December 2008 / Accepted: 15 April 2009 / Published online: 29 April 2009

Abstract Electrodeposition of nanostructured titanium–nickel films was performed and the effect of the concentration of the titanium source on the film characteristics was investigated. Scanning electron microscopy indicated circular crystallites on the surface of the electrodeposited titanium–nickel film with a fairly uniform size distribution. XRD studies showed that the electrodeposited TiNi films contained TiNi with a preferred crystallographic orientation of [002]. Surface analysis using X-ray photoelectron spectroscopy (XPS) revealed that the electrodeposited titanium–nickel film contained elemental titanium and nickel, hydroxide of nickel, and oxides of titanium and nickel. As the titanium ion concentration was increased, the titanium content in the film was increased while the deposition rate and crystallite size of the film were decreased. A blue-shift in the UV/Vis peak was also observed with increasing titanium ion concentration.

Introduction

Titanium–nickel (TiNi) films have attractive properties, including shape memory effect, superelasticity, high damping capacity, good chemical resistance, and biocompatibility [1, 2]. These properties make TiNi films excellent candidates as smart and functional materials [3]. In addition, TiNi thin films have drawn considerable attention in the field of microelectromechanical systems (MEMS) because standard lithography techniques can also be easily adapted to pattern the TiNi films [4–6].

TiNi films are typically fabricated by sputter deposition [4, 5]. However, this method requires a vacuum system, which makes it complicated and expensive. In addition, sputtered TiNi films are quite sensitive to the process conditions such as the target power, gas pressure, target-to-substrate distance, substrate bias, deposition temperature, etc. [2]. Other methods such as laser ablation [7], flash evaporation [8], ion beam deposition [9], and plasma ion implantation [10] have also been used to deposit TiNi films. However, these methods have some intrinsic problems such as nonuniform film thickness and composition as well as low-deposition rates [2].

On the other hand, electrodeposition is a simple way of depositing metallic films because it can be done at atmospheric pressure [11–16]. It offers relatively high-deposition rates and good control over the film compositions [17, 18]. In particular, the crystallite size of a film can be controlled easily during electrodeposition. Control of the crystallite size is of primary importance because the crystallite size affects the resistivity and structural stability of nanostructured films [19, 20]. However, there are no reports on the electrodeposition of TiNi films in the literature.

In this study, a bath was developed for the electrodeposition of nanostructured TiNi films. The effect of the concentration of the Ti source on the composition and deposition rate of the electrodeposited TiNi film was examined. Control of the crystallite size of the film was realized by simply varying the concentration of the Ti source.

H.-M. Lee · S. K. Mahapatra · J. K. Anthony · F. Rotermund · C.-K. Kim (✉)
Division of Energy Systems Research, Ajou University, San 5 Woncheon-dong, Yeongtong-gu, Suwon 443-749, Korea
e-mail: changkoo@ajou.ac.kr

Present Address:
S. K. Mahapatra
Department of Applied Physics, Birla Institute of Technology, Mesra, Ranchi 835215, India

Experimental

TiNi films were electrodeposited on indium tin oxide (ITO)-coated glass substrates using a potentiostatic method. Titanium oxysulfate ($TiOSO_4$) and nickel sulfate ($NiSO_4$) were used as the sources of titanium and nickel, respectively. Tri-sodium citrate (TSC) was used as a complexing agent at a concentration of 0.01 M. The concentration of $TiOSO_4$ ranged from 0.005 to 0.03 M while the concentration of $NiSO_4$ was fixed to 0.01 M throughout the study. The electrolytes were obtained by dissolving the above chemicals in deionized water. The pH of the electrolytes was 3 ± 0.01. Prior to electrodeposition of the TiNi films, the electrolytes were deaerated with nitrogen gas.

Electrodeposition was carried out using a standard three-electrode cell. A platinum-coated titanium mesh (2.5 cm^2 in size) and a saturated Ag/AgCl electrode were used as a counter electrode and a reference electrode, respectively. The substrate was an ITO-coated glass wafer. The wafer was cut into a 1×3 cm^2 rectangle and lacquered to expose 1 cm^2 for electrodeposition of the TiNi films. The substrate was cleaned by blowing with nitrogen gas before deposition. Deposition was carried out at a constant potential of -1.2 V versus Ag/AgCl from a stagnant electrolyte at room temperature (23 ± 2 °C) for 30 s. After deposition, the samples were washed with a water jet and dried with flowing nitrogen gas.

The electrochemical measurements were conducted using a computer-controlled potentiostat (Princeton Applied Research, VSP). The film thickness was measured using a surface profiler (Ambios Technology, XP-1). The SEM images were obtained with a field emission scanning electron microscope (FE-SEM) (Hitachi, S-4800). Surface compositional analysis was carried out by X-ray photoelectron spectroscopy (XPS) (ThermoVG, Sigma probe). The X-ray source of 1486.6 eV was generated using a moveable Al anode (monocromated) at 15 kV. Microstructure analysis of the nanostructured TiNi films was carried out using a high power X-ray diffractometer (Rigaku, D/max-2500/PC), which used a Cu K_α radiation (wave length = 0.154 nm) as an incident beam and worked at 0.02°, 40 kV, and 150 mA. The linear absorption of the films was measured using UV/Vis spectroscopy (Jasco-V530).

Results and discussion

Figure 1 shows the typical Ni 2*p* and Ti 2*p* X-ray photoemission spectra of nanostructured TiNi films electrodeposited from an electrolyte containing 0.01 M $TiOSO_4$, 0.01 M $NiSO_4$, and 0.01 M TSC. The nanostructured TiNi films obtained using different $TiOSO_4$ concentrations (0.005, 0.02, and 0.03 M) had similar XPS spectra to that shown in Fig. 1. In Fig. 1a, the peak at binding energy of 852.3 eV corresponds to elemental nickel, while the peaks at 853.6 and 855.8 eV indicate the presence of hydroxide and oxide of nickel in the film, respectively. The Ti 2*p* spectrum (Fig. 1b) shows peaks for Ti^{4+} ions at 458.4 eV and titanium oxides at 464.3 eV.

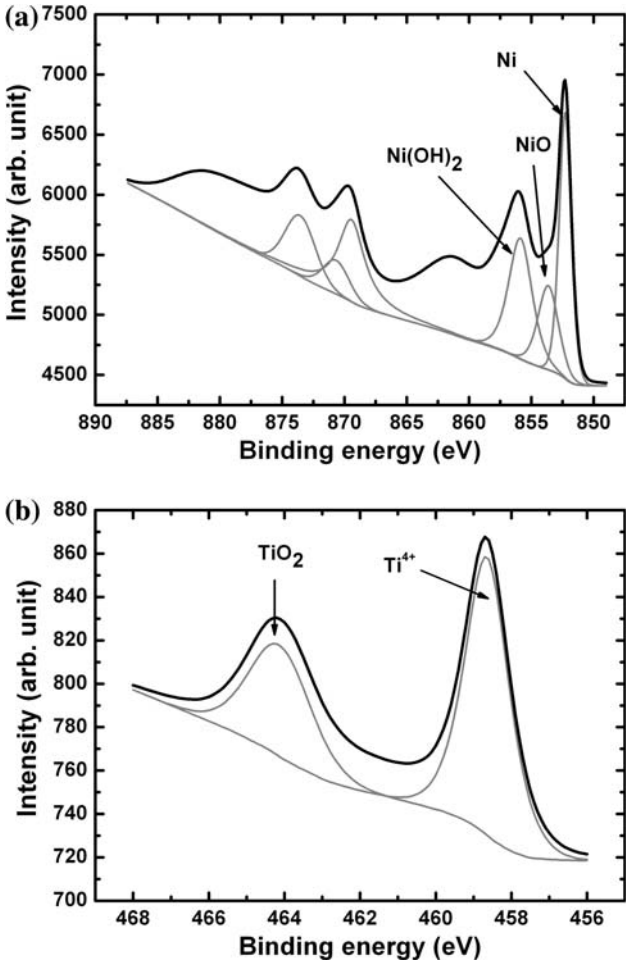

Fig. 1 **a** Ni 2*p* and **b** Ti 2*p* X-ray photoemission spectra of the nanostructured TiNi films deposited by electrodeposition. The concentrations of titanium oxysulfate and nickel sulfate were 0.01 M each. Deconvolution (thin gray lines) of the spectra was carried out using a linear background and Gaussian functions

The composition of the nanostructured TiNi film could be obtained from the areas under the deconvoluted peaks of the XPS spectra. Figure 2 shows the film composition at various titanium ion concentrations. It is seen that the nanostructured TiNi films contains mainly Ni under the deposition conditions employed in this study. The titanium content increased from 7 to 27 at.% when the concentration of its precursor in the electrolyte ranged from 0.005 to 0.03 M.

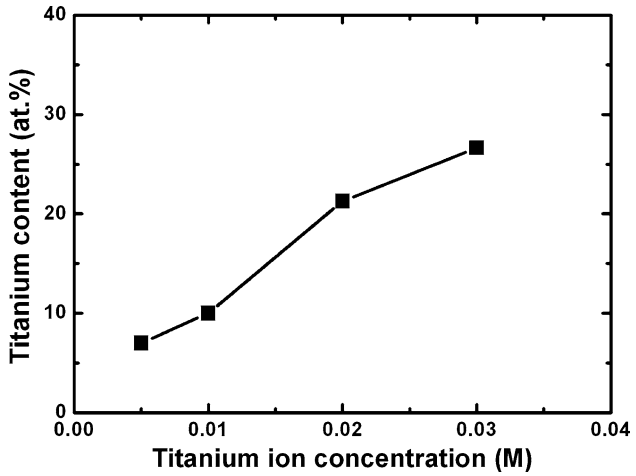

Fig. 2 Titanium content in the nanostructured TiNi films as a function of titanium ion concentration. The nickel sulfate concentration was 0.01 M

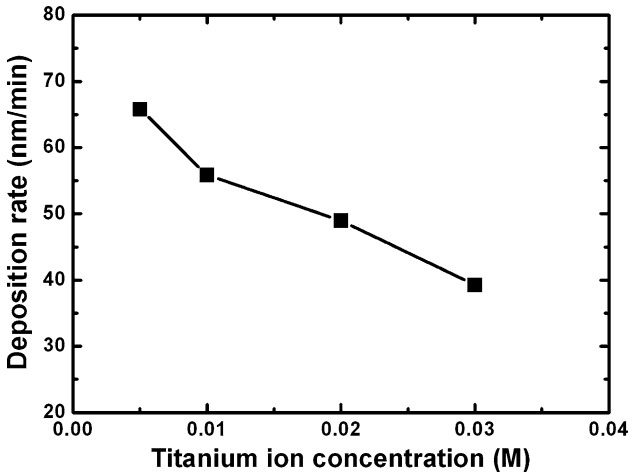

Fig. 4 Deposition rate of the nanostructured TiNi films as a function of titanium ion concentration. The nickel sulfate concentration was 0.01 M

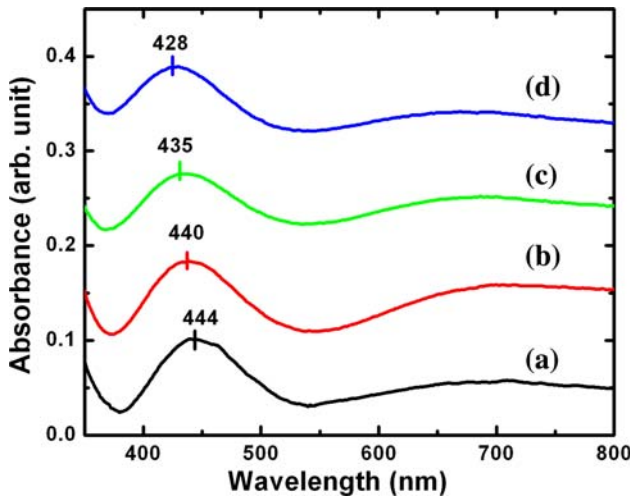

Fig. 3 Linear absorption spectra of the nanostructured TiNi films electrodeposited at titanium ion concentrations of (*a*) 0.005, (*b*) 0.01, (*c*) 0.02, and (*d*) 0.03 M. The nickel sulfate concentration was 0.01 M. The surface plasmon absorption peaks are denoted

A change in the composition of the nanostructured TiNi films at various concentrations of the titanium ion was also observed by measuring the surface plasmon resonance absorption, as shown in Fig. 3. The absorption peak was clearly seen at the wavelength of approximately 430 nm, indicating that a TiNi film had been deposited. A blue-shift in the absorption peak from 444 to 428 nm was observed with increasing titanium ion concentration. It is known that a shift in a surface plasmon resonance peak depends on the atomic composition of bimetallic films [21, 22]. Therefore, the variation of titanium ion concentrations resulted in the compositional change of the nanostructured TiNi films and, in turn, a shift in a surface plasmon resonance peak.

Figure 4 shows the effect of the titanium ion concentration on the deposition rate of nanostructured TiNi films measured using a surface profiler. The deposition rate decreased with increasing titanium ion concentration. The reason why the deposition rate of the TiNi film decreased with increasing titanium ion concentration appears to have resulted from the inhibitive action of titanium ions on the electrodeposition of TiNi.

It was reported that during the electrodeposition of some bimetallic alloys consisting transition metals, one of the constituent elements was deposited through a two-step reduction. For example, electrodeposition of a CoW alloy occurs through the electrochemical reduction of tungstate ions to tungstate oxide and then chemical reduction of tungstate oxide to metallic tungsten [23]. Due to the two-step reduction of tungstate ions to elemental tungsten, the addition of tungstate ions to a cobalt-containing solution inhibits electrodeposition, resulting in a decrease in film thickness with tungstate ion concentration [24].

Robin et al. [25] proposed that electrodeposition of titanium films using fluoride melts occurred through two reduction steps. Although the titanium source used in this study was $TiOSO_4$, it is still expected that titanium was electrodeposited through a two-step reduction process. Therefore, the deposition rate of the TiNi film decreased with increasing titanium ion concentration.

Figure 5 shows the SEM images of the nanostructured TiNi films electrodeposited at various concentrations of the titanium ion. The surface morphology suggests that the films contain circular crystallites with a fairly uniform size. The average crystallite size decreased with increasing titanium ion concentration, showing that the addition of titanium ions inhibits the electrodeposition of TiNi films.

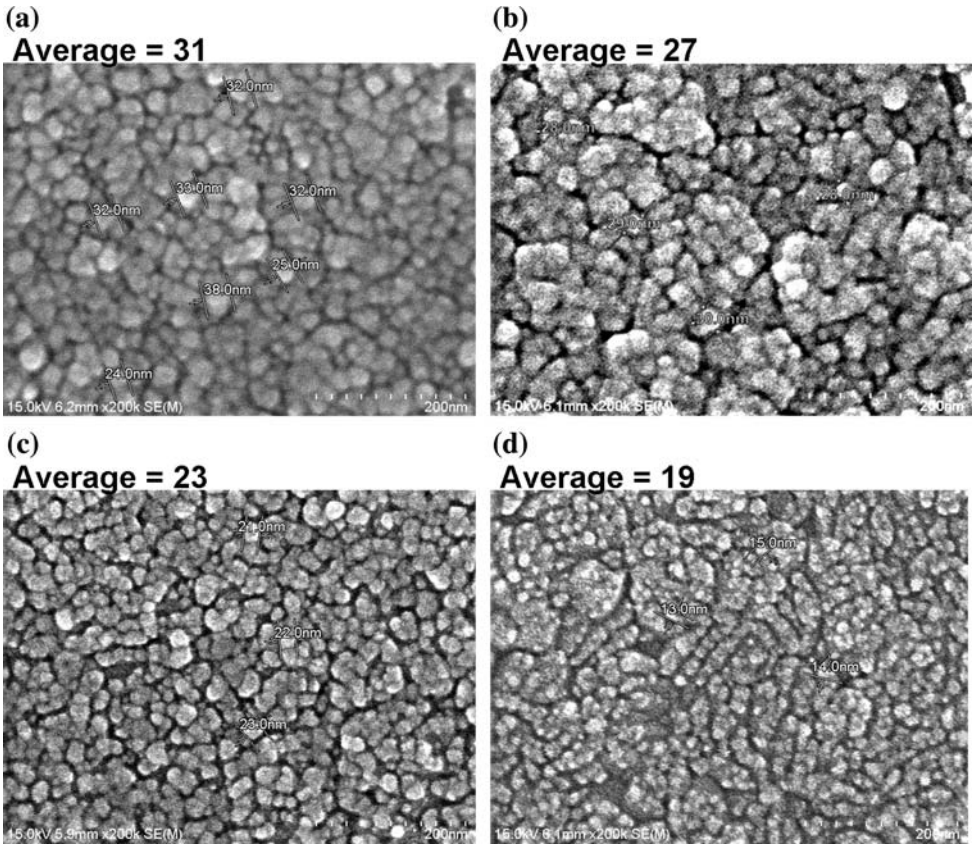

Fig. 5 SEM images of nanostructured TiNi films electrodeposited at titanium oxysulfate concentrations of **a** 0.005, **b** 0.01, **c** 0.02, and **d** 0.03 M. The nickel sulfate concentration was 0.01 M. The unit for the numbers shown in the SEM images is nm

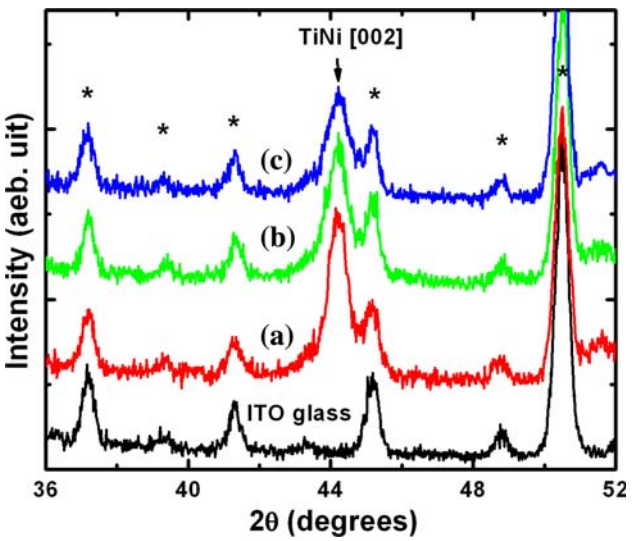

Fig. 6 XRD spectra of the nanostructured TiNi films electrodeposited at titanium ion concentrations of (*a*) 0.01, (*b*) 0.02, and (*c*) 0.03 M. The nickel sulfate concentration was 0.01 M. The XRD pattern of the ITO-glass substrate is also included. *Stars* (*) represent peaks related to In_2O_3

Figure 6 shows X-ray diffraction patterns of the nanostructured TiNi films electrodeposited from electrolytes of various titanium ion concentrations. The XRD pattern of the ITO-glass substrate is also included in Fig. 6. A diffractogram of the ITO-glass substrate shows peaks at $2\theta = 37.2°$, 39.4°, 41.3°, 45.2°, 48.8°, and 50.5°, which are related to In_2O_3. XRD patterns of the electrodeposited TiNi films show a peak at $2\theta = 44.2°$, which is due to TiNi with a crystallographic orientation of [002].

The average grain size of the nanostructured TiNi films electrodeposited from electrolytes of various titanium ion concentrations are calculated from the Debye–Scherrer equation [26],

$$D = \frac{K\lambda}{\beta \cos\theta}$$

where D is the grain size, K is the Scherrer constant, λ is the wavelength of X-ray, β is the full width at half maximum (FWHM), and θ is the diffraction angle. Using the Debye–Scherrer equation, the grain size of the electrodeposited TiNi films was plotted as a function of titanium ion concentration as shown in Fig. 7. The grain size decreases with increasing titanium ion concentration, similarly to the results obtained with SEM measurements. In addition, the values of the grain size determined from the Debye–Scherrer equation are very close to those measured from the SEM images.

Conclusions

Nanostructured TiNi films were electrodeposited from an electrolyte containing $TiOSO_4$, nickel sulfate, and TSC.

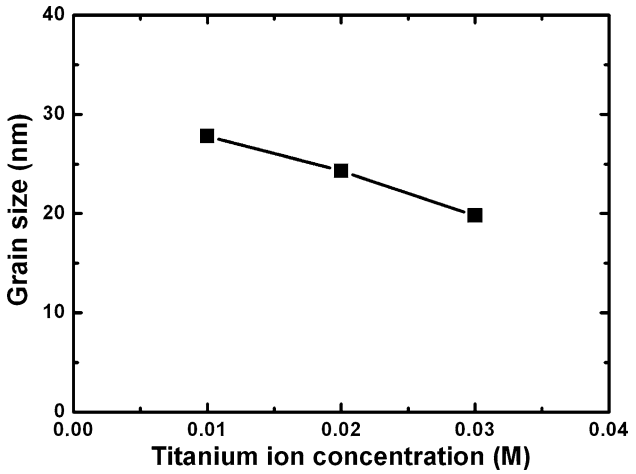

Fig. 7 Grain size of the nanostructured TiNi films as a function of titanium ion concentration. The nickel sulfate concentration was 0.01 M

XPS analysis of the surface of the electrodeposited TiNi films showed that the film contained elemental Ti and Ni as well as hydroxide of Ni and oxides of Ti and Ni. The composition of the nanostructured TiNi films consisted mainly of Ni with a Ti content increasing with titanium ion concentration. A blue-shift in the UV/Vis peak with increasing titanium ion concentration was observed, resulting from the compositional change of the nanostructured TiNi films with titanium ion concentration.

The change in the titanium ion concentration affected the deposition rate and crystallite size of the electrodeposited TiNi films, in that both the deposition rate and crystallite size of the film decreased with increasing titanium ion concentration. This was attributed to the inhibitive action of titanium ions on the electrodeposition of TiNi films.

The surface morphology of the nanostructured TiNi films showed that the films contained circular crystallites with a fairly uniform size distribution. XRD studies showed that the electrodeposited TiNi films contained TiNi with a preferred crystallographic orientation of [002].

These results highlight the feasibility of fabricating nanostructured TiNi films by electrodeposition and offer a simple way of controlling the crystallite size of TiNi films.

Acknowledgements This work was supported by the Basic Research Program of the Korea Science and Engineering Foundation (Grant No. R01-2006-000-11264-0), an Ajou University Research Fellowship 2007 (Grant No. 20072650), and Eugene Technology, Ltd.

References

1. Humbeeck JV (1999) Mater Sci Eng A 273–275:134
2. Fu Y, Du H, Huang W, Zhang S, Hu M (2004) Sens Actuator A 112:395
3. Ishida A, Martynov V (2002) MRS Bull 27:111
4. Krulevitch P, Lee AP, Ramsey PB, Trevino JC, Hamilton J, Northrup MA (1996) J Microelectromech Syst 5:270
5. Kahn H, Huff MA, Heuer AH (1998) J Micromech Microeng 8:213
6. Miyazaki S, Ishida A (1999) Mater Sci Eng A 273–275:106
7. Li C, Nikumb S, Wong F (2006) Opt Lasers Eng 44:1078
8. Makino E, Uenoyama M, Shibata T (1998) Sens Actuator A 71:187
9. Castro AT, Cuellar EL, Mendez UO, Yacaman MJ (2008) Mater Sci Eng A 481–482:476
10. Tan L, Crone WC (2002) Acta Mater 50:4449
11. Nourmohammadi A, Bahrevar MA, Schulze S, Hietschold (2008) J Mater Sci 43:4753. doi:10.1007/s10853-008-2665-3
12. Xu J, Xu Y (2008) J Mater Sci 43:4163. doi:10.1007/s10853-006-1222-1
13. Kaneko Y, Sakakibara H, Hashimoto S (2008) J Mater Sci 43:3931. doi:10.1007/s10853-007-2371-6
14. Leska B, Pankiewicz R, Gierczyk B, Schroeder G, Brzezinski B (2008) J Mater Sci 43:3459. doi:10.1007/s10853-007-2279-1
15. Bhuiyan MS, Talyor BJ, Paranthaman M, Thompson JR, Sinclair JW (2008) J Mater Sci 43:1644. doi:10.1007/s10853-007-2383-2
16. Tu WY, Xu BS, Dong SY, Wang HD, Bin J (2008) J Mater Sci 43:1102. doi:10.1007/s10853-007-2259-5
17. Dulal SMSI, Yoon HJ, Shin CB, Kim CK (2007) J Electrochem Soc 154:D494
18. Dulal SMSI, Yoon HJ, Shin CB, Kim CK (2007) Electrochim Acta 53:934
19. Gleiter H (2000) Acta Mater 48:1
20. Hosseini M, Yasaei B (1998) Ceram Int 24:543
21. Hostetler MJ, Zhong CJ, Yen BKH, Anderegg J, Gross SM, Evans ND, Porter M, Murray RW (1998) J Am Chem Soc 120:9396
22. Sangpour P, Akhavan O, Moshfegh AZ (2007) Appl Surf Sci 253:7438
23. Ibrahim MAM, Rehim SSA, Moussa SO (2003) J Appl Electrochem 33:627
24. Dulal SMSI, Shin CB, Sung JY, Kim CK (2008) J Appl Electrochem 38:83
25. Robin A, de Lepinay J, Barbier MJ (1987) J Electroanal Chem 230:125
26. Petterson AL (1939) Phys Rev 56:978